

# Preclinical Evaluation of Minigastrin Analogs and Proof-of-Concept [<sup>68</sup>Ga]Ga-DOTA-CCK-66 PET/CT in 2 Patients with Medullary Thyroid Cancer

Thomas Günther\*<sup>1</sup>, Nadine Holzleitner\*<sup>1</sup>, Oliver Viering<sup>2</sup>, Roswitha Beck<sup>1</sup>, Georgine Wienand<sup>2</sup>, Alexander Dierks<sup>2</sup>, Christian H. Pfob<sup>2</sup>, Ralph A. Bundschuh<sup>2</sup>, Malte Kircher<sup>2</sup>, Constantin Lapa<sup>2</sup>, and Hans-Jürgen Wester<sup>1</sup>

<sup>1</sup>Department of Chemistry, Chair of Pharmaceutical Radiochemistry, TUM School of Natural Sciences, Technical University of Munich, Garching, Germany; and <sup>2</sup>Nuclear Medicine, Faculty of Medicine, University of Augsburg, Augsburg, Germany

Because of the need for radiolabeled theranostics for the detection and treatment of medullary thyroid cancer (MTC), and the yet unresolved stability issues of minigastrin analogs targeting the cholecystokinin-2 receptor (CCK-2R), our aim was to address in vivo stability, our motivation being to develop and evaluate DOTA-CCK-66 (DOTA-γ-glu-PEG<sub>3</sub>-Trp-(N-Me)Nle-Asp-1-Nal-NH<sub>2</sub>, PEG: polyethylene glycol) and DOTA-CCK-66.2 (DOTA-glu-PEG<sub>3</sub>-Trp-(N-Me)Nle-Asp-1-Nal-NH<sub>2</sub>), both derived from DOTA-MGS5 (DOTA-glu-Ala-Tyr-Gly-Trp-(N-Me)Nle-Asp-1-Nal-NH<sub>2</sub>), and clinically translate [<sup>68</sup>Ga]Ga-DOTA-CCK-66. **Methods:** <sup>64</sup>Cu and <sup>67</sup>Ga labeling of DOTA-CCK-66, DOTA-CCK-66.2, and DOTA-MGS5 was performed at 90°C within 15 min (1.0 M NaOAc buffer, pH 5.5, and 2.5 M 4-(2-hydroxyethyl)-1-piperazineethanesulfonic acid buffer, respectively). <sup>177</sup>Lu labeling of these 3 compounds was performed at 90°C within 15 min (1.0 M NaOAc buffer, pH 5.5, 0.1 M sodium ascorbate). CCK-2R affinity of <sup>nat</sup>Ga/<sup>nat</sup>Cu/<sup>nat</sup>Lu-labeled DOTA-CCK-66, DOTA-CCK-66.2, and DOTA-MGS5 was examined on AR42J cells. The in vivo stability of <sup>177</sup>Lu-labeled DOTA-CCK-66 and DOTA-MGS5 was examined at 30 min after injection in CB17-SCID mice. Biodistribution studies at 1 h (<sup>67</sup>Ga]Ga-DOTA-CCK-66) and 24 h (<sup>177</sup>Lu]Lu-DOTA-CCK-66/DOTA-MGS5) after injection were performed on AR42J tumor-bearing CB17-SCID mice. In a translation to the human setting, [<sup>68</sup>Ga]Ga-DOTA-CCK-66 was administered and whole-body PET/CT was acquired at 120 min after injection in 2 MTC patients. **Results:** Irrespective of the metal or radiometal used (copper, gallium, lutetium), high CCK-2R affinity (half-maximal inhibitory concentration, 3.6–6.0 nM) and favorable lipophilicity were determined. In vivo, increased numbers of intact peptide were found for [<sup>177</sup>Lu]Lu-DOTA-CCK-66 compared with [<sup>177</sup>Lu]Lu-DOTA-MGS5 in murine urine (23.7% ± 9.2% vs. 77.8% ± 2.3%). Overall tumor-to-background ratios were similar for both <sup>177</sup>Lu-labeled analogs. [<sup>67</sup>Ga]Ga-DOTA-CCK-66 exhibited accumulation (percentage injected dose per gram) that was high in tumor (19.4 ± 3.5) and low in off-target areas (blood, 0.61 ± 0.07; liver, 0.31 ± 0.02; pancreas, 0.23 ± 0.07; stomach, 1.81 ± 0.19; kidney, 2.51 ± 0.49) at 1 h after injection. PET/CT examination in 2 MTC patients applying [<sup>68</sup>Ga]Ga-DOTA-CCK-66 confirmed multiple metastases. **Conclusion:** Because of the high in vivo stability and favorable overall preclinical performance of [<sup>nat</sup>/<sup>67</sup>Ga]Ga-/[<sup>nat</sup>/<sup>177</sup>Lu]Lu-DOTA-CCK-66, a proof-of-concept clinical investigation of [<sup>68</sup>Ga]Ga-DOTA-CCK-66 was completed. As several lesions could be identified and excellent biodistribution patterns were observed, further patient studies applying [<sup>68</sup>Ga]Ga- and [<sup>177</sup>Lu]Lu-DOTA-CCK-66 are warranted.

For correspondence or reprints, contact Thomas Günther (thomas.guenther@tum.de).

\*Contributed equally to this work.

**Key Words:** DOTA-CCK-66; clinical translation; CCK-2R; medullary thyroid cancer

**J Nucl Med 2024; 65:33–39**

DOI: 10.2967/jnumed.123.266537

**D**espite progress in cancer treatment, metastasis still accounts for more than 90% and remains the primary cause of cancer death (1). For medullary thyroid cancer (MTC), which accounts for less than 3% of all thyroid cancers, the 10-y survival rate for patients who already had distant metastases at initial diagnosis was only 40% (2,3). Because of the limited role of conventional therapies in metastatic MTC not amenable to local treatment (4,5), and given the fact that tyrosine kinase inhibitors including antiangiogenic as well as selective RET (rearranged during transfection) inhibitors—though effective—can cause significant toxicity or induce resistance (6,7), alternative treatment options for early detection of MTC are needed. Elevated basal calcitonin plasma levels are common in MTC patients and can be measured after calcium or pentagastrin stimulation testing (8,9). Patients with confirmed elevated calcitonin levels usually undergo PET imaging using, for example, 3,4-dihydroxy-6-[<sup>18</sup>F]fluoro-L-phenylalanine ([<sup>18</sup>F]F-DOPA), given the neuroendocrine origin of MTC cells (10). Despite good detection rates using [<sup>18</sup>F]F-DOPA PET/CT for primary and metastatic MTC, an even improved sensitivity at lower calcitonin levels would be desirable (11–13). Moreover, even if metastases are accurately identified by [<sup>18</sup>F]F-DOPA PET/CT, there is no therapeutic analog available for this compound for subsequent radioligand therapy.

The cholecystokinin-2 receptor (CCK-2R) has been shown to be overexpressed on most MTC cells, thus promoting the development of several different compounds addressing this target over the last few years (14–18). CCK-2R ligands carrying a DOTA chelator can be used for imaging (<sup>68</sup>Ga-labeled) or radioligand therapy (<sup>177</sup>Lu-labeled)—an advantage over [<sup>18</sup>F]F-3,4-dihydroxyphenylalanine (DOPA). Apart from <sup>68</sup>Ga, <sup>64</sup>Cu could be an interesting alternative for PET imaging because of its favorable half-life (12.7 h) and positron energy (653 keV), enabling later imaging time points and high spatial resolution (19). However, the low metabolic stability of minigastrin derivatives targeting CCK-2R is still a problem that affects therapeutic efficacy. Several cleavage sites were reported for minigastrin analogs (Tyr-Gly, Gly-Trp, and Asp-Phe) (20), of which some were chemically addressed in DOTA-MGS5 (DOTA-glu-Ala-Tyr-Gly-Trp-(N-Me)Nle-Asp-1-Nal-NH<sub>2</sub>, Fig. 1) (21). In vivo

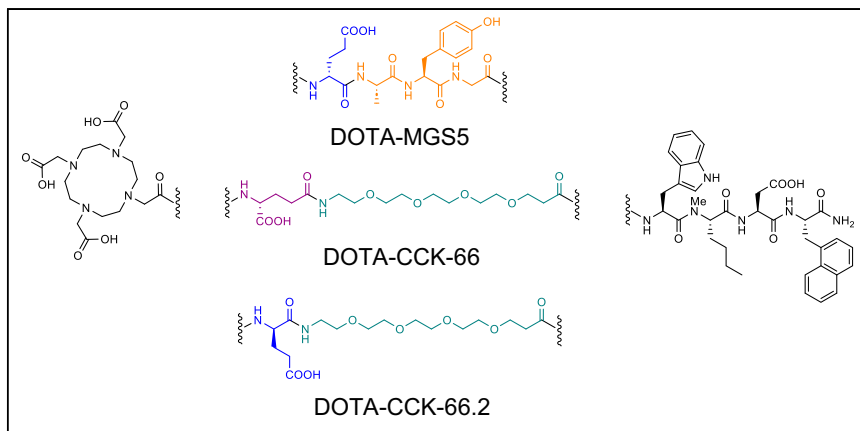


**FIGURE 1.** Chemical structures of compounds evaluated. All comprise same C-terminal tetrapeptide binding motif and N-terminal DOTA chelator but differ in linker section. Orange = Ala-Tyr-Gly sequence; green = PEG<sub>3</sub> moiety; blue =  $\alpha$ -bridged D-glutamic acid moiety; violet =  $\gamma$ -bridged D-glutamic acid moiety.

properties in animals and first patient data thus looked promising for [<sup>68</sup>Ga]Ga-DOTA-MGS5 (21,22).

However, particularly the cleavage sites Tyr-Gly and Gly-Trp are still not addressed in this compound. Therefore, we recently reported on a series of CCK-2R ligands in which we substituted the N-terminal L-amino acids in DOTA-MGS5 (H-glu-Ala-Tyr-Gly) by simple polyethylene glycol (PEG) linkers. Interestingly, we observed a lower in vitro stability in human serum (23), although the introduction of PEG linkers usually increases stability (24). Because negative charges at the N-terminus of minigastrin analogs seem to increase metabolic stability (25), we introduced either a  $\gamma$ -D-glutamic acid ( $\gamma$ -glu) or a  $\alpha$ -D-glutamic acid (glu) moiety between the DOTA chelator and the PEG<sub>3</sub> linker of DOTA-CCK-64 (DOTA-PEG<sub>3</sub>-Trp-(N-Me)Nle-Asp-1-Nal-NH<sub>2</sub>), which resulted in DOTA-CCK-66 (DOTA- $\gamma$ -glu-PEG<sub>3</sub>-Trp-(N-Me)Nle-Asp-1-Nal-NH<sub>2</sub>) and DOTA-CCK-66.2 (DOTA-glu-PEG<sub>3</sub>-Trp-(N-Me)Nle-Asp-1-Nal-NH<sub>2</sub>) (Fig. 1). Furthermore, this study aimed to elucidate whether this simple modification could tackle the stability issues observed in previous studies. Hence, a comparative preclinical evaluation of DOTA-CCK-66, DOTA-CCK-66.2, and DOTA-MGS5, each labeled with [<sup>nat/64</sup>Cu]copper, [<sup>nat/67</sup>Ga]gallium, or [<sup>nat/177</sup>Lu]lutetium, encompassed the determination of CCK-2R affinity (half-maximal inhibitory concentration [IC<sub>50</sub>]) on AR42J cells, lipophilicity (expressed as n-octanol/phosphate-buffered saline distribution coefficient [ $\log D_{7,4}$ ]), human serum albumin binding, in vivo stability, and biodistribution studies on AR42J tumor-bearing mice. Moreover, we selected [<sup>68</sup>Ga]Ga-DOTA-CCK-66 for proof-of-concept PET/CT examinations in 2 MTC patients.

## MATERIALS AND METHODS

### Synthesis and Labeling Procedures

Precursor synthesis was conducted via solid-phase peptide synthesis using an H-Rink Amide ChemMatrix resin (loading, 0.55 mmol/g; Sigma-Aldrich Chemie GmbH). Characterization of all compounds is provided in Supplemental Figures 1–9 (supplemental materials are available at <http://jnm.snmjournals.org>). Purification was accomplished via reversed-phase high-performance liquid chromatography (RP-HPLC).

<sup>64</sup>Cu- and <sup>177</sup>Lu-labeling of DOTA-CCK-66, DOTA-CCK-66.2, and DOTA-MGS5 was completed using an established protocol (26). <sup>67</sup>Ga-labeling of these 3 compounds was performed analogously using 4-(2-hydroxyethyl)-1-piperazineethanesulfonic acid (2.5 M in H<sub>2</sub>O) buffer. Detailed descriptions of all labeling procedures (<sup>nat/68</sup>Ga, <sup>nat/64</sup>Cu,

<sup>nat/177</sup>Lu) are provided in the supplemental materials. [<sup>64</sup>Cu]CuCl<sub>2</sub> was purchased from DSD-Pharma GmbH. [<sup>67</sup>Ga]GaCl<sub>3</sub> was acquired from Curium. [<sup>177</sup>Lu]LuCl<sub>3</sub> was purchased from ITM Isotope Technologies Munich SE.

The synthesis of [<sup>68</sup>Ga]Ga-DOTA-CCK-66 for human PET/CT studies was completed in agreement with good manufacturing practices using a good-radiopharmaceutical-practice module (Scintomics GmbH) equipped with an SC-01 gallium peptide labeling kit (ABX). [<sup>68</sup>Ga]GaCl<sub>3</sub> was obtained from a <sup>68</sup>Ge/<sup>68</sup>Ga-generator (GalliAD; IRE Elit Radiopharma). A 900 ± 300 MBq activity of the <sup>68</sup>Ga-eluate was combined with a solution of the DOTA-CCK-66 precursor (50  $\mu$ g) and NaOAc buffer in the reactor and heated. Afterward, the solution was transferred onto a Sep-Pak C18 Light cartridge (Waters) for purification. The cartridge was washed with water and eluted with

ethanol, and the solution was diluted with phosphate-buffered saline. Subsequently, sterile filtration was completed using a Millex-GV filter (Merck KGaA). Quality control was conducted using thin-layer chromatography (NH<sub>4</sub>OAc/MeOH; Agilent) and HPLC measurement against the corresponding reference compound, [<sup>nat</sup>Ga]Ga-DOTA-CCK-66. Furthermore, a sterile filter integrity test, a limulus amoebocyte lysate, and a postapplication sterility test were performed.

### In Vitro Experiments

The CCK-2R affinity (by means of IC<sub>50</sub>) of <sup>nat</sup>Ga/<sup>nat</sup>Cu/<sup>nat</sup>Lu-labeled DOTA-CCK-66, DOTA-CCK-66.2, and DOTA-MGS5 and the  $\log D_{7,4}$  of <sup>67</sup>Ga/<sup>64</sup>Cu/<sup>177</sup>Lu-labeled DOTA-CCK-66, DOTA-CCK-66.2, and DOTA-MGS5 were determined according to a published procedure (27). Human serum albumin binding of <sup>nat</sup>Ga/<sup>nat</sup>Cu/<sup>nat</sup>Lu-labeled DOTA-CCK-66, DOTA-CCK-66.2, and DOTA-MGS5 was determined by high-performance affinity chromatography (Supplemental Fig. 10), as previously reported (28,29). In vitro stability studies of <sup>177</sup>Lu-labeled DOTA-CCK-66, DOTA-CCK-66.2, and DOTA-MGS5 in human serum were completed in analogy to a published procedure (30). A detailed description of in vitro experiments is provided in the supplemental materials.

### In Vivo Experiments

**Animal Experiments.** All animal experiments were approved by the General Administration of Upper Bavaria (ROB-55.2-1-2532.Vet\_02-18-109) and completed using a previously published protocol (26). All animal studies were in compliance with the ARRIVE (Animal Research: Reporting of In Vivo Experiments) guidelines (supplemental materials).

In vivo stability studies at 30 min after intravenous injection ( $n = 3$ ) were completed according to a published procedure using about 30–40 MBq (1 nmol) of [<sup>177</sup>Lu]Lu-DOTA-CCK-66 and [<sup>177</sup>Lu]Lu-DOTA-MGS5, respectively, for each animal (26).

For biodistribution studies, approximately 2–4 MBq (100 pmol, 150  $\mu$ L) of [<sup>67</sup>Ga]Ga-DOTA-CCK-66, [<sup>177</sup>Lu]Lu-DOTA-CCK-66, or [<sup>177</sup>Lu]Lu-DOTA-MGS5 were injected into the tail vein of anesthetized (2% isoflurane) 2- to 3-mo-old female AR42J tumor-bearing CB17-SCID mice ( $n = 4$ ). Organs were removed and weighed, and the accumulated radioactivity was measured in a  $\gamma$ -counter (Perkin Elmer) after euthanasia at 1 h (<sup>67</sup>Ga-labeled) and 24 h (<sup>177</sup>Lu-labeled) after injection.

Imaging studies using [<sup>67</sup>Ga]Ga-DOTA-CCK-66, [<sup>177</sup>Lu]Lu-DOTA-CCK-66, or [<sup>177</sup>Lu]Lu-DOTA-MGS5 were performed according to a

published protocol (26). Static images were recorded at  $t = 1$  and 24 h after injection (anesthesia by 2% isoflurane,  $n = 1$ ) with an acquisition time of  $t + (45\text{--}60 \text{ min})$  using a high-energy general-purpose rat and mouse collimator via MILabs acquisition software versions 11.00 and 12.26 from MILabs.

For competition studies ( $n = 2$ ), a 3.03 mg/kg concentration (40 nmol) of [ $^{nat}\text{Ga}$ ]Ga-DOTA-MGS5 ( $10^{-3} \text{ M}$  in phosphate-buffered saline) was coinjected with [ $^{67}\text{Ga}$ ]Ga-DOTA-CCK-66 (100 pmol), or a 3.25 mg/kg concentration (40 nmol) of [ $^{nat}\text{Lu}$ ]Lu-DOTA-MGS5 ( $10^{-3} \text{ M}$  in phosphate-buffered saline) was coadministered with [ $^{177}\text{Lu}$ ]Lu-DOTA-CCK-66 (100 pmol).

Acquired data were statistically analyzed using the Student *t*-test via Excel (Microsoft Corp.) and OriginPro software (version 9.7; OriginLab Corp.). Acquired *P* values of less than 0.05 were considered statistically significant.

**Clinical PET/CT.** [ $^{68}\text{Ga}$ ]Ga-DOTA-CCK-66 was applied for restaging purposes in 2 MTC patients (male, aged 64 y, and female, aged 46 y). Both patients presented with rising calcitonin levels and calcitonin doubling times shorter than 24 mo at the time of PET/CT imaging, indicating tumor progression. Before CCK-2R-directed imaging, [ $^{18}\text{F}$ ]F-DOPA PET/CT had been negative in both subjects, prompting further diagnostic work-up. The application is allowed by the German Medical Act (§13 2b Arzneimittelgesetz), which waives the need for institutional review board approval. Both patients gave written informed consent after receiving comprehensive medical information from a board-certified nuclear medicine physician. All procedures were completed in accordance with the Declaration of Helsinki and its later amendments and the legal considerations of clinical guidelines. The ethical compliance of this approach was confirmed by the local Ethics Committee of Ludwig-Maximilians-Universität München (approval 23-0627).

A detailed description of the patients' histories is provided in the supplemental materials. Both patients underwent [ $^{68}\text{Ga}$ ]Ga-DOTA-CCK-66 whole-body imaging using a PET/CT scanner (Biograph mCT 40; Siemens Healthineers) at 120 min after injection of 151 and 193 MBq of [ $^{68}\text{Ga}$ ]Ga-DOTA-CCK-66 ( $\sim 18 \mu\text{g}$  each), respectively. Whole-body CT imaging was performed as auxiliary CT (120 kVp, 40 mAs). PET datasets were reconstructed using a standard protocol provided by the manufacturer (2 iterations, 21 subsets), corrected for randoms, scatter, decay, and attenuation (using whole-body auxiliary CT).

## RESULTS

### Synthesis and Radiolabeling

The synthesized precursors were obtained in yields of 3%–7% (chemical purity  $> 95\%$ ) after RP-HPLC purification. Labeling using a 2.5-fold excess of [ $^{nat}\text{Ga}$ ]Ga( $\text{NO}_3$ ) $_3$ , [ $^{nat}\text{Lu}$ ]LuCl $_3$ , or [ $^{nat}\text{Cu}$ ]Cu(OAc) $_2$  resulted in quantitative yields. No purification step was conducted before in vitro experiments, as no effects of free metal ions on overall affinity data was observed in previous experiments (26).  $^{177}\text{Lu}$ ,  $^{67}\text{Ga}$ , and  $^{64}\text{Cu}$  labeling of DOTA-CCK-66, DOTA-CCK-66.2, and DOTA-MGS5 was performed manually, each resulting in radiochemical yields and purities of more than 95% and molar activities of 10–50 GBq/ $\mu\text{mol}$  (non-decay-corrected). All compounds were used without further purification.

The synthesized batches of [ $^{68}\text{Ga}$ ]Ga-DOTA-CCK-66 used for proof-of-concept studies in 2 MTC patients yielded  $150 \pm 50 \text{ MBq}$  ( $\sim 56\%$  non-decay-corrected). All specifications were fulfilled. The pH of the 16-mL solution was 7.5. Both the  $^{nat}\text{Ga}$ -labeled reference compound and the  $^{68}\text{Ga}$ -labeled product showed the same retention times using RP-HPLC. The radiochemical purity determined by

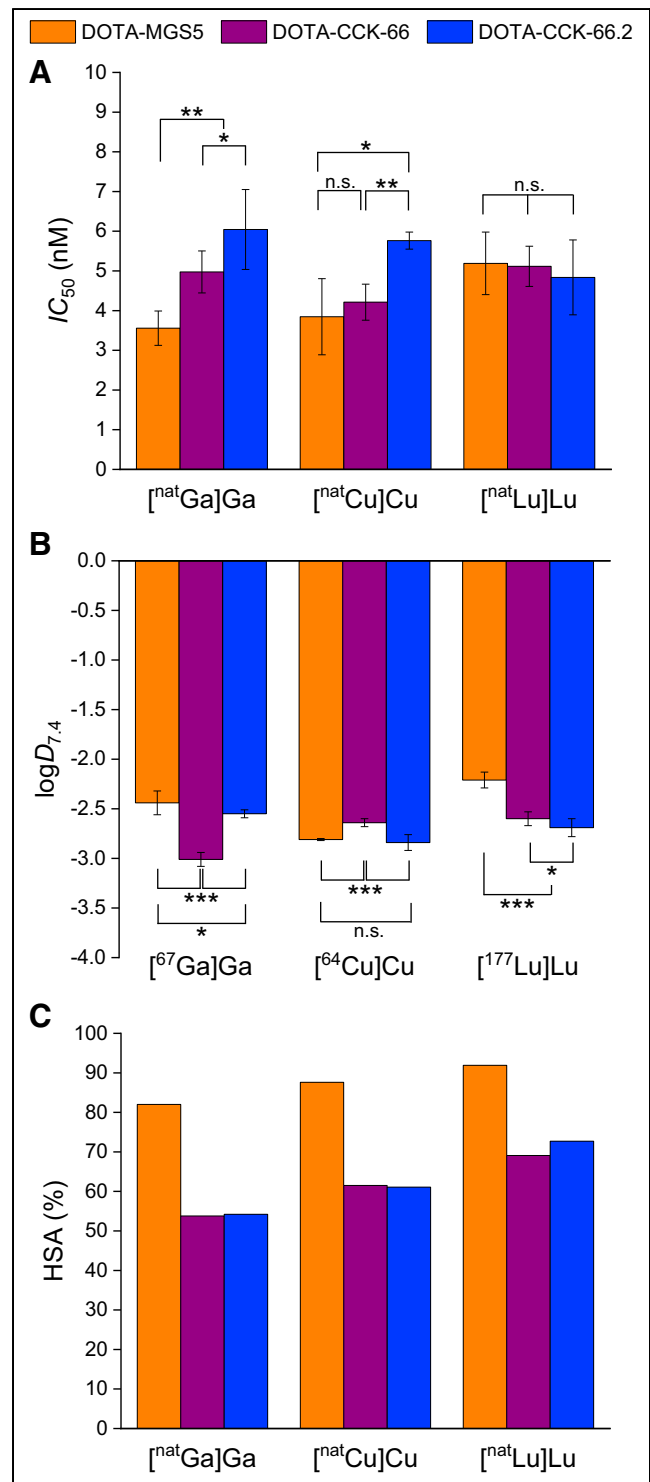


**FIGURE 2.** In vitro data of  $^{nat/64}\text{Cu}$ -,  $^{nat/67}\text{Ga}$ -, and  $^{nat/177}\text{Lu}$ -labeled CCK-2R ligands. Data are expressed as mean  $\pm$  SD. (A) Affinity data ( $n = 3$ ) on AR42J cells ( $2.0 \times 10^5$  cells per well) using [ $^{177}\text{Lu}$ ]Lu-DOTA-PP-F11N (0.3 pmol/well) as radiolabeled reference (3 h, 37°C, RPMI 1640, 5 mM L-Gln, 5 mL nonessential amino acids [ $\times 100$ ], 10% fetal calf serum + 5% bovine serum albumin [ $v/v$ ]). (B)  $\log D_{7,4}$  ( $n = 6$ ). (C) Human serum albumin binding as determined by high-performance affinity chromatography. n.s. = not significant. \* $P < 0.05$ . \*\* $P < 0.01$ . \*\*\* $P < 0.0001$ .

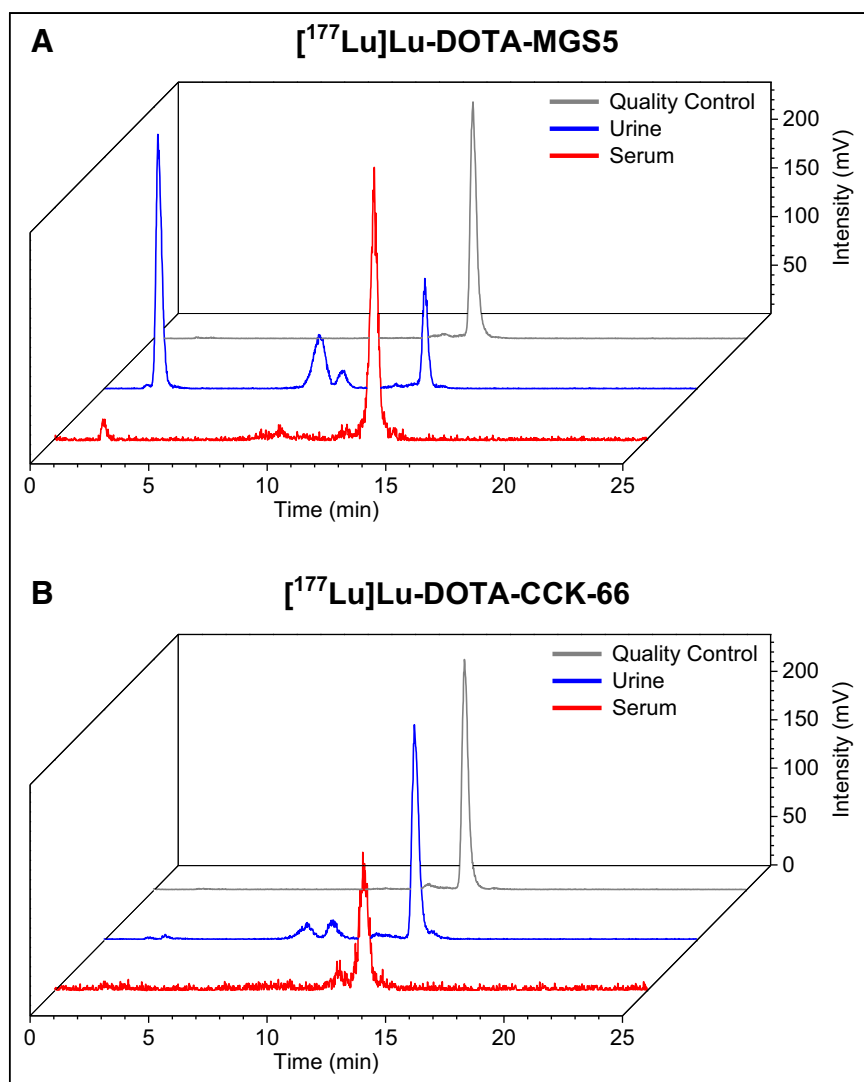


**FIGURE 3.** In vivo stability of CCK-2R ligands: amount of intact compound at 30 min after injection (3 each) in murine serum (red) and urine (blue) for [ $^{177}\text{Lu}$ ]Lu-DOTA-MGS5 (A) and [ $^{177}\text{Lu}$ ]Lu-DOTA-CCK-66 (B) (quality control in gray).

RP-HPLC was higher than 95%, and the content of unbound [ $^{68}\text{Ga}$ ]Ga species was less than 0.8%. Thin-layer chromatography measurement also revealed less than 0.8% of unbound [ $^{68}\text{Ga}$ ]Ga $^{3+}$ .

#### In Vitro Characterization

All 3 compounds exhibited high CCK-2R affinity on AR42J cells ( $\text{IC}_{50}$ , 3.6–6.0 nM, irrespective of whether  $^{\text{nat}}\text{Ga}$ -,  $^{\text{nat}}\text{Cu}$ -, or  $^{\text{nat}}\text{Lu}$ -labeled; Fig. 2A; Supplemental Table 1). [ $^{\text{nat}}\text{Ga}$ ]Ga-DOTA-MGS5 revealed significantly lower  $\text{IC}_{50}$  values than [ $^{\text{nat}}\text{Ga}$ ]Ga-DOTA-CCK-66 and -66.2 ( $P < 0.004$ ), and [ $^{\text{nat}}\text{Cu}$ ]Cu-DOTA-CCK-66.2 displayed significantly higher  $\text{IC}_{50}$  values than [ $^{\text{nat}}\text{Cu}$ ]Cu-DOTA-MGS5 and [ $^{\text{nat}}\text{Cu}$ ]Cu-DOTA-CCK-66 ( $P < 0.03$ ). Distribution coefficients ( $\log D_{7.4}$ ) were in the range of  $-3.0$  to  $-2.2$  for all 3 ligands, independent of whether  $^{67}\text{Ga}$ -,  $^{64}\text{Cu}$ -, or  $^{177}\text{Lu}$ -labeled (Fig. 2B, Supplemental Table 1). [ $^{67}\text{Ga}$ ]Ga-DOTA-CCK-66 revealed significantly lower  $\log D_{7.4}$  values than [ $^{67}\text{Ga}$ ]Ga-DOTA-MGS5 and [ $^{67}\text{Ga}$ ]Ga-DOTA-CCK-66.2 ( $P < 0.0001$ ), [ $^{64}\text{Cu}$ ]Cu-DOTA-CCK-66 exhibited significantly higher  $\log D_{7.4}$  values than [ $^{64}\text{Cu}$ ]Cu-DOTA-MGS5 and [ $^{64}\text{Cu}$ ]Cu-DOTA-CCK-66.2 ( $P < 0.0001$ ), and

[ $^{177}\text{Lu}$ ]Lu-DOTA-MGS5 displayed significantly higher  $\log D_{7.4}$  values than [ $^{177}\text{Lu}$ ]Lu-DOTA-CCK-66 and -66.2 ( $P < 0.0001$ ). Both DOTA-CCK-66 and DOTA-CCK-66.2 exhibited distinctly lower human serum albumin binding than DOTA-MGS5, irrespective of the radiometal used (Fig. 2C; Supplemental Table 2). In vitro stability studies in human serum ( $37^\circ\text{C}$ , 72 h) showed comparable numbers of intact tracer for all 3  $^{177}\text{Lu}$ -labeled CCK-2R ligands (Supplemental Fig. 11, Supplemental Table 3). Because of the overall similar, but slightly more favorable, in vitro properties of DOTA-CCK-66 (independent of the metals used), DOTA-CCK-66.2 was excluded from further experiments.

#### In Vivo Characterization

In total, 25 animals were used for in vivo stability ( $2 \times 3$ ), biodistribution ( $3 \times 4$ ), imaging ( $3 \times 1$ ), and competition ( $2 \times 2$ ) studies. Intact compound was similar between [ $^{177}\text{Lu}$ ]Lu-DOTA-CCK-66 and [ $^{177}\text{Lu}$ ]Lu-DOTA-MGS5 in murine serum ( $78.5\% \pm 3.1\%$  vs.  $82.0\% \pm 0.1\%$ ) at 30 min after injection but was higher for [ $^{177}\text{Lu}$ ]Lu-DOTA-CCK-66 than for [ $^{177}\text{Lu}$ ]Lu-DOTA-MGS5 in the urine ( $77.8\% \pm 2.3\%$  vs.  $23.7\% \pm 9.2\%$ ,  $P < 0.001$ ) (Fig. 3). Biodistribution studies on AR42J tumor-bearing mice revealed high initial tumor uptake ( $19.4 \pm 3.5$  percentage injected dose per gram [%ID/g]) for [ $^{67}\text{Ga}$ ]Ga-DOTA-CCK-66, whereas off-target accumulation in all organs was less than 2.6 %ID/g at 1 h after injection (Fig. 4A; Supplemental Table 4). At 24 h after injection, [ $^{177}\text{Lu}$ ]Lu-DOTA-CCK-66 displayed slightly lower activity levels in the tumor than did [ $^{177}\text{Lu}$ ]Lu-DOTA-MGS5 ( $8.6 \pm 1.1$  %ID/g vs.  $11.0 \pm 1.2$  %ID/g,  $P < 0.02$ ) but also slightly lower off-target activity

retention in most organs (stomach,  $P < 0.01$ ), which resulted in comparable tumor-to-background ratios overall (Supplemental Tables 4 and 5).

Imaging studies (Fig. 4B) corroborated the biodistribution profiles well, revealing high activity levels in the tumor and low levels in all organs for [ $^{67}\text{Ga}$ ]Ga-DOTA-CCK-66 (1 h after injection), as well as for [ $^{177}\text{Lu}$ ]Lu-DOTA-CCK-66 and [ $^{177}\text{Lu}$ ]Lu-DOTA-MGS5 (24 h after injection). Competition studies of both [ $^{67}\text{Ga}$ ]Ga-DOTA-CCK-66 (1 h after injection) and [ $^{177}\text{Lu}$ ]Lu-DOTA-CCK-66 (24 h after injection) using an excess of [ $^{\text{nat}}\text{Ga}$ ]Ga-/[ $^{\text{nat}}\text{Lu}$ ]Lu-DOTA-MGS5 confirmed specificity of tumor uptake (Supplemental Fig. 12; Supplemental Table 4).

Because of its overall in vitro and in vivo properties [ $^{68}\text{Ga}$ ]Ga-DOTA-CCK-66 was selected for proof-of-concept PET/CT application in 2 MTC patients.

#### Proof-of-Concept Study in Humans

[ $^{68}\text{Ga}$ ]Ga-DOTA-CCK-66-PET showed a favorable biodistribution, with the highest uptake in tumor lesions and the CCK-2R-expressing stomach. Besides the kidneys, ureters, and bladder



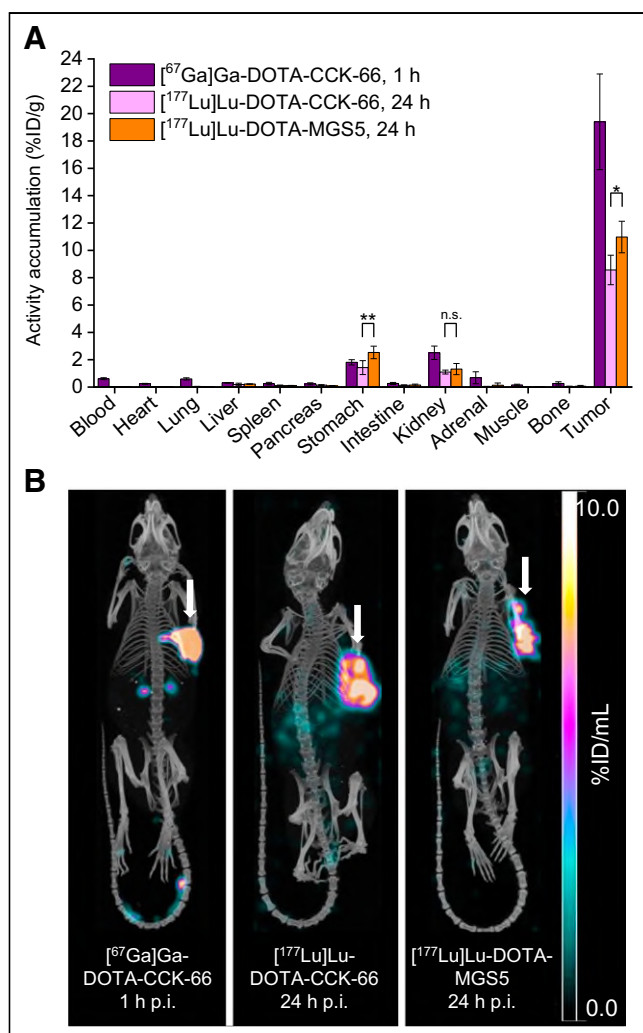


**FIGURE 4.** (A) Biodistribution of [<sup>67</sup>Ga]Ga-DOTA-CCK-66 (1 h after injection), as well as [<sup>177</sup>Lu]Lu-DOTA-CCK-66 and [<sup>177</sup>Lu]Lu-DOTA-MGS5 (24 h after injection), in selected organs in AR42J tumor-bearing CB17-SCID mice (100 pmol each). Data are %ID/g (mean ± SD, 4 each). (B) Maximum-intensity projection of AR42J tumor (arrows)-bearing CB17-SCID mice (1 each) injected with [<sup>67</sup>Ga]Ga-DOTA-CCK-66, as well as [<sup>177</sup>Lu]Lu-DOTA-CCK-66 and [<sup>177</sup>Lu]Lu-DOTA-MGS5 (100 pmol each). Images were acquired at either 1 or 24 h after injection. n.s. = not significant; p.i. = after injection. \**P* < 0.05. \*\**P* < 0.01.

(due to excretion), no significant activity levels were found in other organs. [<sup>68</sup>Ga]Ga-DOTA-CCK-66 was well tolerated, and no side effects or changes in vital signs were observed during the tracer's slow intravenous injection (~2 min) or thereafter (with a follow-up period of 4 h).

A 64-y-old male patient who had initially undergone thyroidectomy and cervical lymph node dissection had a long history of disease, with several local and lymph node recurrences, and presented at the time of PET/CT imaging with a rising calcitonin level of 110 pg/mL and a calcitonin doubling time of 16 mo. On [<sup>68</sup>Ga]Ga-DOTA-CCK-66 PET/CT, suggestive CCK-2R-expressing lymph nodes were detected in the left retroclavicular region and in the upper mediastinum (Fig. 5). Subsequently, the lymph nodes were surgically resected and histologically confirmed as lymph node metastases of MTC.

A 46-y-old female patient who had undergone thyroidectomy and cervical lymph node dissection, as well as external-beam

radiation of the thyroid bed due to local tumor remnants, showed a rising calcitonin level of 380 pg/mL and a calcitonin doubling time of 5 mo at the time of PET/CT imaging. [<sup>68</sup>Ga]Ga-DOTA-CCK-66 detected several lymph node metastases (bilaterally hilar, right retroclavicular), liver metastases (in both liver lobes), and bone metastases (atlas, right eighth rib, right femur, right os ischii) (Fig. 6). In comparison to the [<sup>18</sup>F]FDG PET/CT available for this patient, [<sup>68</sup>Ga]Ga-DOTA-CCK-66 detected additional lymph node, liver, and bone metastases.

## DISCUSSION

Because of the ongoing need for novel and improved treatment options for MTC patients, several CCK-2R ligands have been reported over the last few years, particularly compounds addressing the stability issues of minigastrin derivatives by chemical design (15–18). In our group, we developed a series of radiohybrid-based minigastrin analogs that revealed a high activity accumulation in the tumor but also suffered from elevated kidney retention due to the presence of a silicon-fluoride acceptor moiety and several negative charges within the linker section (27,30). Therefore, we recently focused on shorter CCK-2R ligands and aimed to address metabolic stability by the introduction of PEG linkers, which, however, resulted in a lower stability (23). To address this matter in this study, we made some minor modifications within the linker sequence of our minigastrin derivatives and completed in vitro and in vivo evaluations, as well as initiating clinical translation of our most favorable compound.

Synthesis of the precursors was easily accessible via solid-phase peptide synthesis, and complexation proceeded quantitatively, irrespective of the metal or radiometal used. Because of their structural similarity, both novel compounds and the reference peptide, DOTA-MGS5, revealed a comparable CCK-2R affinity and favorable  $\log D_{7.4}$ . On the basis of the similar but slightly more favorable in vitro properties of the DOTA-CCK-66 peptide over the DOTA-CCK-66.2 peptide, we excluded the latter from further evaluation.

In vivo stability at 30 min after injection was comparable for both [<sup>177</sup>Lu]Lu-DOTA-CCK-66 and [<sup>177</sup>Lu]Lu-DOTA-MGS5 in murine serum but distinctly different in murine urine, as the former revealed a 3-fold higher amount of intact compound than the reference. This finding suggests that [<sup>177</sup>Lu]Lu-DOTA-CCK-66 is cleared from the blood mostly intact whereas [<sup>177</sup>Lu]Lu-DOTA-MGS5 is cleared predominantly metabolized. Because of their structural similarity, this beneficial property can be attributed to the introduction of a  $\gamma$ -glu moiety between the DOTA and the PEG<sub>3</sub> linker, because a previous compound that differed from DOTA-CCK-66 only by the absence of this  $\gamma$ -glu unit exhibited a noticeably lower stability (23). The amount of intact peptide in the urine even surpassed that of a recently reported CCK-2R ligand, [<sup>177</sup>Lu]Lu-DOTA-(GABOB)<sub>2</sub>- $\beta$ -Ala-Trp-(N-Me)Nle-Asp-1-Nal-NH<sub>2</sub>, which also substituted N-terminal amino acids by unnatural moieties and revealed high in vivo stability (77.8% ± 2.3% vs. ~60%) (16).

Because of its high metabolic stability, [<sup>67</sup>Ga]Ga-DOTA-CCK-66 demonstrated a high accumulation of activity in the tumor at 1 h after injection, whereas off-target accumulation was either low or cleared rapidly, resulting in low activity levels in all organs, even in the CCK-2R-expressing stomach. Hence, favorable tumor-to-background ratios were determined and were approximately 2-fold higher in all organs than reported for [<sup>68</sup>Ga]Ga-DOTA-MGS5 (21). The more rapid clearance rates corroborate the distinctly lower human

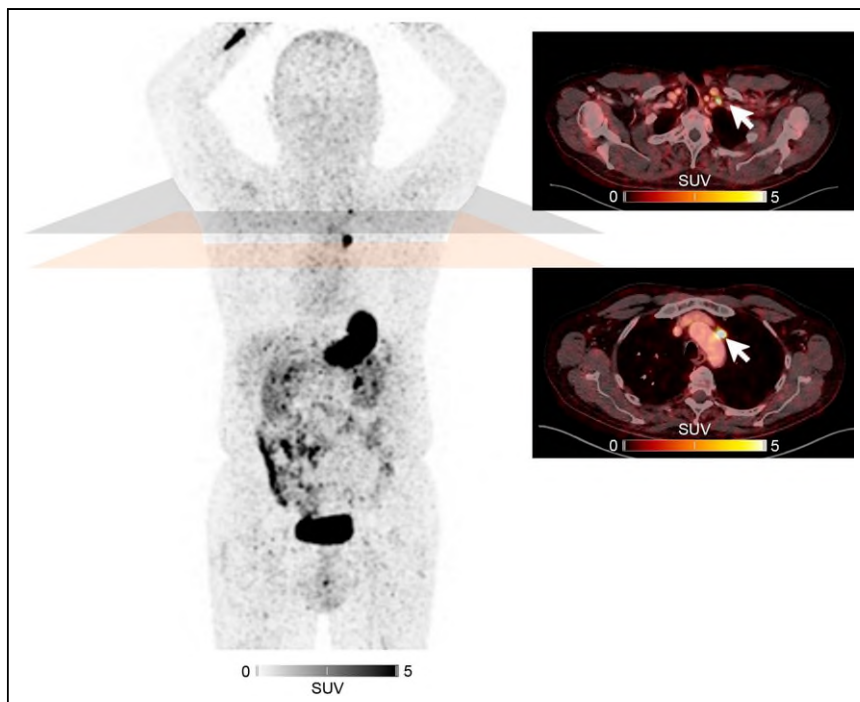


**FIGURE 5.** Maximum-intensity projection (left) and fused transaxial slices (right) of 64-y-old male MTC patient undergoing PET/CT at 2 h after intravenous injection of 151 MBq of [ $^{68}\text{Ga}$ ]Ga-DOTA-CCK-66. CCK-2R-expressing lymph node metastases could be detected in left retroclavicular region and in upper mediastinum (arrows).

serum albumin binding observed by high-performance affinity chromatography, a finding that might be responsible for the favorably low activity uptake overall (apart from the tumor). The comparison of [ $^{68}\text{Ga}$ ]Ga-DOTA-MGS5 and [ $^{68}\text{Ga}$ ]Ga-DOTA-CCK-66 is a limitation

of this study, as biodistribution studies of these compounds have been performed by different groups using different mouse models (BALB/c vs. CB17-SCID) and tumor models (A431-CCK2R vs. AR42J), as well as precursor amounts (20 vs. 100 pmol) (21). Comparison of the  $^{177}\text{Lu}$ -labeled analogs at 24 h after injection using the same modalities revealed similar tumor-to-background ratios overall, indicating that [ $^{177}\text{Lu}$ ]Lu-DOTA-MGS5 and [ $^{177}\text{Lu}$ ]Lu-DOTA-CCK-66 might be equivalent in the application for radioligand therapy. However, further clinical investigation is needed.

On the basis of the favorable preclinical data of [ $^{67}\text{Ga}$ ]Ga-DOTA-CCK-66, its  $^{68}\text{Ga}$ -analog was selected for a clinical proof-of-concept investigation. [ $^{68}\text{Ga}$ ]Ga-DOTA-CCK-66 PET/CT on 2 MTC patients at 120 min after injection revealed high uptake in tumor lesions and the physiologically CCK-2R-expressing stomach. Furthermore, off-target accumulation was low, corroborating the biodistribution profiles in mice well. Hence, several lymph node, bone, and liver metastases could be identified in these 2 MTC patients. Interestingly, we could observe a higher tumor-to-organ contrast at 120 min than at 60 min after injection. A similar trend was also reported for [ $^{68}\text{Ga}$ ]Ga-DOTA-MGS5 (22), indicating a slightly decelerated tumor accumulation and a fast off-target clearance of these minigastrin analogs. On the basis of these observations and the similar in vitro properties of [ $^{64}\text{Cu}$ ]Cu-DOTA-CCK-66, PET/CT examinations using [ $^{64}\text{Cu}$ ]Cu-DOTA-CCK-66 could be a viable alternative in the future, since it would enable later imaging time points.

[ $^{68}\text{Ga}$ ]Ga-DOTA-CCK-66 PET/CT did not show any biosafety issues and allows for radioligand therapy using [ $^{177}\text{Lu}$ ]Lu-DOTA-CCK-66, which might represent an advantage of radiolabeled CCK-2R ligands over [ $^{18}\text{F}$ ]FDG or [ $^{18}\text{F}$ ]F-DOPA. On the basis of the fast renal activity clearance and low activity accumulation observed in the kidneys, we do not expect any issues regarding kidney toxicity using [ $^{177}\text{Lu}$ ]Lu- or even [ $^{225}\text{Ac}$ ]Ac-DOTA-CCK-66 for radioligand therapy. However, activity retention in the human stomach was higher than observed in the murine stomach and has to be monitored carefully during the first treatment cycles to prevent toxicity. Furthermore, the fact that the feasibility of [ $^{68}\text{Ga}$ ]Ga-DOTA-CCK-66 has been shown only for single patients to date is a limitation of this study, thus demanding further clinical evaluation of this compound to verify its clinical value.

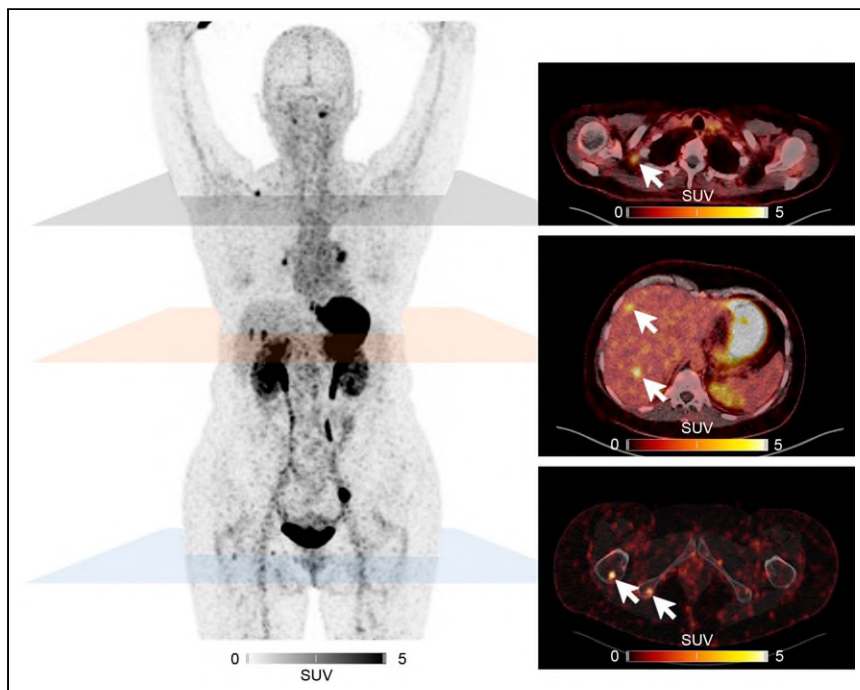


**FIGURE 6.** Maximum-intensity projections (left) and fused transaxial sections (right) of 46-y-old female MTC patient undergoing PET/CT at 2 h after intravenous injection of 193 MBq of [ $^{68}\text{Ga}$ ]Ga-DOTA-CCK-66. Several lymph node (e.g., right retroclavicular), liver, and bone metastases (e.g., right femur and right ischium) could be detected (arrows).

## CONCLUSION

[<sup>67</sup>Ga]Ga-DOTA-CCK-66 revealed excellent preclinical characteristics, particularly high in vivo stability and rapid activity clearance, thus providing good tumor-to-background ratios. A proof-of-concept investigation on 2 MTC patients using [<sup>68</sup>Ga]Ga-DOTA-CCK-66 PET/CT showed favorable biodistribution patterns and identified several lesions, which could be histopathologically confirmed as metastases of MTC. One advantage of this compound over the MTC imaging gold standard, [<sup>18</sup>F]F-DOPA, is the possibility for <sup>177</sup>Lu labeling for subsequent radioligand therapy. Therefore, additional patient studies using [<sup>68</sup>Ga]Ga- or [<sup>64</sup>Cu]Cu-DOTA-CCK-66, as well as [<sup>177</sup>Lu]Lu- or even [<sup>225</sup>Ac]Ac-DOTA-CCK-66, are warranted to elucidate the clinical value of this theranostic tool.

## DISCLOSURE

This study was funded by Deutsche Forschungsgemeinschaft (DFG, German Research Foundation—461577150). Thomas Günther received the 2023 Sanjiv Sam Gambhir–Philips and the 2023 Translational Research and Applied Medicine fellowship for support at Stanford University. A patent application on CCK-2R–targeted compounds including DOTA-CCK-66 with Thomas Günther, Nadine Holzleitner, Constantin Lapa, and Hans-Jürgen Wester as inventors has been filed. Hans-Jürgen Wester is founder and shareholder of Scintomics GmbH, Munich, Germany. No other potential conflict of interest relevant to this article was reported.

## KEY POINTS

**QUESTION:** Can a simplistic design modification of the clinically applied CCK-2R ligand [<sup>68</sup>Ga]Ga-DOTA-MGS5 improve preclinical and clinical characteristics?

**PERTINENT FINDINGS:** [<sup>64</sup>Cu]Cu-/[<sup>67</sup>Ga]Ga-/[<sup>177</sup>Lu]Lu-DOTA-CCK-66 displayed similar in vitro and in vivo properties to the reference compound but a noticeably improved in vivo stability, which resulted in favorable activity clearance and, thus, tumor-to-organ contrast in animals and proof-of-concept [<sup>68</sup>Ga]Ga-DOTA-CCK-66 PET/CT applications.

**IMPLICATIONS FOR PATIENT CARE:** Although further [<sup>68</sup>Ga]Ga-DOTA-CCK-66 PET/CT (and [<sup>177</sup>Lu]Lu-/[<sup>225</sup>Ac]Ac-DOTA-CCK-66 for treatment) applications in MTC patients have to be completed, these preliminary results suggest a promising theranostic candidate for clinical use.

## REFERENCES

1. Ganesh K, Massagué J. Targeting metastatic cancer. *Nat Med*. 2021;27:34–44.
2. Thyroid cancer: statistics. Cancer.net website. <https://www.cancer.net/cancer-types/thyroid-cancer/statistics#:~:text=In%202023%2C%20an%20estimated%2043%2C720,with%20thyroid%20cancer%20in%202020>. Published August 2023. Accessed October 30, 2023.
3. Roman S, Lin R, Sosa JA. Prognosis of medullary thyroid carcinoma: demographic, clinical, and pathologic predictors of survival in 1252 cases. *Cancer*. 2006;107:2134–2142.
4. Stamatakis M, Paraskeva P, Stefanaki C, et al. Medullary thyroid carcinoma: the third most common thyroid cancer reviewed. *Oncol Lett*. 2011;2:49–53.
5. Wells SA Jr, Asa SL, Dralle H, et al. Revised American Thyroid Association guidelines for the management of medullary thyroid carcinoma. *Thyroid*. 2015;25:567–610.
6. Vodopivec DM, Hu MI. RET kinase inhibitors for RET-altered thyroid cancers. *Ther Adv Med Oncol*. 2022;14:17588359221101691.
7. Hadoux J, Schlumberger M. Chemotherapy and tyrosine-kinase inhibitors for medullary thyroid cancer. *Best Pract Res Clin Endocrinol Metab*. 2017;31:335–347.
8. Karges W, Dralle H, Raue F, et al. Calcitonin measurement to detect medullary thyroid carcinoma in nodular goiter: German evidence-based consensus recommendation. *Exp Clin Endocrinol Diabetes*. 2004;112:52–58.
9. Hennessy JF, Wells SAJ, Ontjes DA, Cooper CW. A comparison of pentagastrin injection and calcium infusion as provocative agents for the detection of medullary carcinoma of the thyroid. *J Clin Endocrinol Metab*. 1974;39:487–495.
10. Giovannella L, Treglia G, Iakovou I, Mihailovic J, Verburg FA, Luster M. EANM practice guideline for PET/CT imaging in medullary thyroid carcinoma. *Eur J Nucl Med Mol Imaging*. 2020;47:61–77.
11. Treglia G, Castaldi P, Villani MF, et al. Comparison of <sup>18</sup>F-DOPA, <sup>18</sup>F-FDG and <sup>68</sup>Ga-somatostatin analogue PET/CT in patients with recurrent medullary thyroid carcinoma. *Eur J Nucl Med Mol Imaging*. 2012;39:569–580.
12. Brammen L, Niederle MB, Riss P, et al. Medullary thyroid carcinoma: do ultrasonography and F-DOPA-PET-CT influence the initial surgical strategy? *Ann Surg Oncol*. 2018;25:3919–3927.
13. Terroir M, Caramella C, Borget I, et al. F-18-dopa positron emission tomography/computed tomography is more sensitive than whole-body magnetic resonance imaging for the localization of persistent/recurrent disease of medullary thyroid cancer patients. *Thyroid*. 2019;29:1457–1464.
14. von Guggenberg E, Kolenc P, Rottenburger C, Mikolajczak R, Hubalewska-Dydejczyk A. Update on preclinical development and clinical translation of cholecystokinin-2 receptor targeting radiopharmaceuticals. *Cancers (Basel)*. 2021;13:5776.
15. Zavvar TS, Hörmann AA, Klingler M, et al. Effects of side chain and peptide bond modifications on the targeting properties of stabilized minigastrin analogs. *Pharmaceuticals (Basel)*. 2023;16:278.
16. Hörmann AA, Klingler M, Rangger C, et al. Effect of N-terminal peptide modifications on in vitro and in vivo properties of <sup>177</sup>Lu-labeled peptide analogs targeting CCK2R. *Pharmaceuticals*. 2023;15:796.
17. Grob NM, Schibli R, Behe M, Valverde IE, Mindt TL. 1,5-disubstituted 1,2,3-triazoles as amide bond isosteres yield novel tumor-targeting minigastrin analogs. *ACS Med Chem Lett*. 2021;12:585–592.
18. Sauter AW, Mansi R, Hassiepen U, et al. Targeting of the cholecystokinin-2 receptor with the minigastrin analog <sup>177</sup>Lu-DOTA-PP-F11N: does the use of protease inhibitors further improve in vivo distribution? *J Nucl Med*. 2019;60:393–399.
19. Braune A, Oehme L, Freudenberg R, et al. Comparison of image quality and spatial resolution between <sup>18</sup>F, <sup>68</sup>Ga, and <sup>64</sup>Cu phantom measurements using a digital Biograph Vision PET/CT. *EJNMMI Phys*. 2022;9:58.
20. Ocak M, Helbok A, Rangger C, et al. Comparison of biological stability and metabolism of CCK2 receptor targeting peptides, a collaborative project under COST BM0607. *Eur J Nucl Med Mol Imaging*. 2011;38:1426–1435.
21. Klingler M, Summer D, Rangger C, et al. DOTA-MGS5, a new cholecystokinin-2 receptor-targeting peptide analog with an optimized targeting profile for theranostic use. *J Nucl Med*. 2019;60:1010–1016.
22. Von Guggenberg E, Uprimny C, Klinger M, et al. Preliminary clinical experience with cholecystokinin-2 receptor PET/CT using the <sup>68</sup>Ga-labeled minigastrin analog DOTA-MGS5 in patients with medullary thyroid cancer. *J Nucl Med*. 2023;64:859–862.
23. Holzleitner N, Günther T, Daoud-Gadieh A, Lapa C, Wester HJ. Investigation of the structure-activity relationship at the N-terminal part of minigastrin analogs. *EJNMMI Res*. 2023;13:65.
24. Khandare J, Minko T. Polymer–drug conjugates: progress in polymeric prodrugs. *Prog Polym Sci*. 2006;31:359–397.
25. Good S, Walter MA, Waser B, et al. Macrocyclic chelator-coupled gastrin-based radiopharmaceuticals for targeting of gastrin receptor-expressing tumours. *Eur J Nucl Med Mol Imaging*. 2008;35:1868–1877.
26. Günther T, Deiser S, Felber V, Beck R, Wester HJ. Substitution of L-tryptophan by a-methyl-L-tryptophan in <sup>177</sup>Lu-RM2 results in <sup>177</sup>Lu-AMTG, a high-affinity gastrin-releasing peptide receptor ligand with improved in vivo stability. *J Nucl Med*. 2022;63:1364–1370.
27. Holzleitner N, Günther T, Beck R, Lapa C, Wester H-J. Introduction of a SiFA moiety into the D-glutamate chain of DOTA-PP-F11N results in radiohybrid-based CCK-2R-targeted compounds with improved pharmacokinetics in vivo. *Pharmaceuticals (Basel)*. 2022;15:1467.
28. Valko K, Nunhuck S, Bevan C, Abraham MH, Reynolds DP. Fast gradient HPLC method to determine compounds binding to human serum albumin. Relationships with octanol/water and immobilized artificial membrane lipophilicity. *J Pharm Sci*. 2003;92:2236–2248.
29. Yamazaki K, Kanaoka M. Computational prediction of the plasma protein-binding percent of diverse pharmaceutical compounds. *J Pharm Sci*. 2004;93:1480–1494.
30. Günther T, Holzleitner N, Di Carlo D, Urtz-Urban N, Lapa C, Wester H-J. Development of the first <sup>18</sup>F-labeled radiohybrid-based minigastrin derivative with high target affinity and tumor accumulation by substitution of the chelating moiety. *Pharmaceuticals*. 2023;15:826.